Published OnlineFirst October 18, 2013; DOI: 10.1158/1535-7163.MCT-13-0466

Cancer Biology and Signal Transduction

Molecular Cancer Therapeutics

Targeting Sphingosine Kinase Induces Apoptosis and Tumor Regression for KSHV-Associated Primary Effusion Lymphoma

Zhiqiang Qin[1,8], Lu Dai[2,8], Jimena Trillo-Tinoco[3], Can Senkal[5], Wenxue Wang[6], Tom Reske[2], Karlie Bonstaff[2], Luis Del Valle[3], Paulo Rodriguez[1], Erik Flemington[4], Christina Voelkel-Johnson[7], Charles D. Smith[6], Besim Ogretmen[5], and Chris Parsons[1,2]

Abstract

Sphingosine kinase (SPHK) is overexpressed by a variety of cancers, and its phosphorylation of sphingosine results in accumulation of sphingosine-1-phosphate (S1P) and activation of antiapoptotic signal transduction. Existing data indicate a role for S1P in viral pathogenesis, but roles for SPHK and S1P in virus-associated cancer progression have not been defined. Rare pathologic variants of diffuse large B-cell lymphoma arise preferentially in the setting of HIV infection, including primary effusion lymphoma (PEL), a highly mortal tumor etiologically linked to the Kaposi's sarcoma-associated herpesvirus (KSHV). We have found that ABC294640, a novel clinical-grade small molecule selectively targeting SPHK (SPHK2 >> SPHK1), induces dose-dependent caspase cleavage and apoptosis for KSHV$^+$ patient-derived PEL cells, in part through inhibition of constitutive signal transduction associated with PEL cell proliferation and survival. These results were validated with induction of PEL cell apoptosis using SPHK2-specific siRNA, as well as confirmation of drug-induced SPHK inhibition in PEL cells with dose-dependent accumulation of proapoptotic ceramides and reduction of intracellular S1P. Furthermore, we demonstrate that systemic administration of ABC294640 induces tumor regression in an established human PEL xenograft model. Complimentary *ex vivo* analyses revealed suppression of signal transduction and increased KSHV lytic gene expression within drug-treated tumors, with the latter validated *in vitro* through demonstration of dose-dependent viral lytic gene expression within PEL cells exposed to ABC294640. Collectively, these results implicate interrelated mechanisms and SPHK2 inhibition in the induction of PEL cell death by ABC294640 and rationalize evaluation of ABC294640 in clinical trials for the treatment of KSHV-associated lymphoma. *Mol Cancer Ther; 13(1); 154–64. ©2013 AACR.*

Introduction

Rare and aggressive pathologic variants of diffuse large B-cell lymphoma (DLBCL) arise more frequently in patients infected with HIV, and the majority of these tumors, including primary effusion lymphoma (PEL), are etiologically linked to the human oncogenic γ-herpesviruses: Kaposi's sarcoma-associated herpesvirus (KSHV) and Epstein–Barr virus (EBV; ref. 1). PEL tumors are causally associated with KSHV, typically infected with both KSHV and EBV (KSHV$^+$EBV$^+$) or KSHV alone (KSHV$^+$EBV^{neg}), arise preferentially within pleural or peritoneal cavities, and progress rapidly despite chemotherapy with a median survival of around 6 months (2–4). Combination cytotoxic chemotherapy represents the current standard of care for PEL (3, 5, 6), but lack of efficacy, off-target effects (including bone marrow suppression), and chemotherapeutic resistance (generated through virus-associated mechanisms) continue to limit the utility of this approach (3, 5–9). A combination of highly active antiretroviral therapy and rituximab, an anti-CD20 monoclonal antibody, has led to short-term responses, but PEL cells generally do not express CD20 (10, 11). The proteasome inhibitor bortezomib and the combination of arsenic trioxide and interferon both reduce NF-κB activation and may work synergistically with cytotoxic chemotherapy to reduce PEL viability (12, 13). Unfortunately, proteasome inhibition and arsenic incur significant toxicities limiting

Authors' Affiliations: Departments of [1]Microbiology, Immunology, and Parasitology, [2]Medicine, and [3]Pathology, Louisiana State University Health Sciences Center, Louisiana Cancer Research Center; [4]Department of Microbiology, Tulane University School of Medicine, New Orleans, Louisiana; Departments of [5]Biochemistry and Molecular Biology, [6]Drug Discovery and Biomedical Sciences, and [7]Microbiology and Immunology, Hollings Cancer Center, Medical University of South Carolina, Charleston, South Carolina; and [8]Research Center for Translational Medicine and Key Laboratory of Arrhythmias, East Hospital, Tongji University School of Medicine, Shanghai, China

Z. Qin and L. Dai contributed equally to this work.

Note: Supplementary data for this article are available at Molecular Cancer Therapeutics Online (http://mct.aacrjournals.org/).

Corresponding Author: Chris Parsons, Suite 712, Louisiana Cancer Research Center, 1700 Tulane Avenue, New Orleans, LA 70112. Phone: 504-210-3328; Fax: 504-210-2927; E-mail: cpars1@lsuhsc.edu

doi: 10.1158/1535-7163.MCT-13-0466

Published OnlineFirst October 18, 2013; DOI: 10.1158/1535-7163.MCT-13-0466

their clinical application. Antiviral agents inhibit γ-herpesvirus replication (14, 15), but these drugs do not affect latent gene expression in PEL cell lines and have limited effects on PEL cell growth *in vitro* (15). Targeting the mammalian target of rapamycin (mTOR) suppresses constitutive signal transduction associated with PEL survival and has proven successful in preclinical models (16), but rapamycin may paradoxically induce activation of alternative signaling pathways, and whether drug concentrations necessary for an antitumoral effect are achievable in patients remains unclear (17). Finally, efficacy data for autologous stem cell transplantation for PEL are also limited, and the problems inherent with additive immune suppression in HIV-infected patients currently preclude routine use of this approach (18). In summary, safer and more effective therapeutic strategies for PEL are urgently needed.

Sphingolipid biosynthesis involves hydrolytic conversion of ceramide to sphingosine, which is subsequently phosphorylated by one of two sphingosine kinase isoforms (SPHK1 or SPHK2) to generate bioactive sphingosine-1-phosphate (S1P; ref. 19). The relative cellular concentrations of ceramide and S1P ultimately determine tumor cell fate, with accumulation of ceramides favoring apoptosis, and accumulation of S1P favoring proliferation (19, 20). SPHK is activated by tumor-promoting cytokines and growth factors, leading to rapid increases in the intracellular levels of S1P and depletion of ceramide species (21). SPHK activity and S1P induce activation of signal transduction, including mitogen-activated protein kinase (MAPK) and NF-κB pathways (22, 23) relevant to KSHV pathogenesis (24, 25), and a small number of studies support a role for sphingolipid biosynthetic pathways in regulation of viral pathogenesis (26, 27). However, functional consequences of targeting SPHK and reducing S1P for virus-infected tumor cells have not been explored.

A novel small molecule, 3-(4-chlorophenyl)-adamantane-1-carboxylic acid (pyridin-4-ylmethyl)amide (ABC294640), inhibits SPHK activity and is highly selective for the SPHK2 isoform at concentrations less than 100 μmol/L (28). ABC294640 displays *in vitro* and *in vivo* activity against a variety of nonviral tumors in preclinical studies, including significant reductions in S1P expression within intratumoral and noncellular fractions (28, 29). In addition, the drug's selectivity for SPHK, evidenced by lack of inhibition of other kinases (30), underscores its observed safety in preclinical studies and, thus far, in a clinical trial enrolling patients with solid tumors (Clinicaltrials.gov identifier, NCT01488513). Therefore, we sought to characterize the impact of ABC294640 inhibition of SPHK for KSHV-infected PEL cell viability *in vitro*, as well as associated tumor progression *in vivo*. In addition, we sought to identify relationships between SPHK inhibition and mechanisms associated with PEL cell death, including induction of apoptosis, accumulation of proapoptotic ceramides, and perturbations in KSHV gene expression.

Materials and Methods

Cell culture and reagents

Body cavity–based lymphoma cells (BCBL-1, $KSHV^+/EBV^{neg}$) and a Burkitt lymphoma cell line (BL-41, $KSHV^{neg}/EBV^{neg}$) were kindly provided by Dr. Dean Kedes (University of Virginia School of Medicine, Charlottesville, VA) and maintained in RPMI 1640 medium (Gibco) with supplements as described previously (31). BC-1 ($KSHV^+/EBV^+$), BC-3 ($KSHV^+/EBV^{neg}$), and BCP-1 ($KSHV^+/EBV^{neg}$) cells were purchased from American Type Culture Collection (ATCC) and maintained in complete RPMI 1640 medium (ATCC) supplemented with 20% FBS. KSHV infection was verified for all cell lines using immunofluorescence assays for detection of the KSHV latency-associated nuclear antigen (LANA). All cells were incubated at 37°C in 5% CO_2. All experiments were carried out using cells harvested at low (<20) passages. The 3-(4-chlorophenyl)-adamantane-1-carboxylic acid (pyridin-4-ylmethyl)amide (ABC294640) was synthesized for all experiments using good laboratory practices as appropriate for clinical applications and previously described (30).

Cell viability assays

Metabolic activity of PEL cells was assessed using standard MTT assays as described previously (31). Apoptosis was quantified by flow cytometry using the fluorescein isothiocyanate (FITC)-annexin V/propidium iodide (PI) Apoptosis Detection Kit I (BD Pharmingen) as previously described (10) and according to the manufacturer's instructions. Data were collected using a FACSCalibur 4-color flow cytometer (BD Bioscience).

Transfection assays

BCBL-1 were transfected using pcDNA3.1-FLAG-ERK, pcDNA3.1-FLAG-NF-κB p65, or control vectors as described previously (32, 33). Transfection efficiency was assessed through cotransfection of a lacZ reporter construct and subsequent determination of β-galactosidase activity using a commercial β-galactosidase enzyme assay system according to the manufacturer's instructions (Promega). For RNA interference (RNAi) assays, SphK2 ON-TARGETplus SMARTpool siRNA (Dharmacon), or negative control siRNA, were delivered using the DharmaFECT transfection reagent according to the manufacturer's instructions. To confirm initial transfection efficiency for siRNA experiments, PEL cells were transfected with GFP-tagged siRNA, and GFP expression was determined by flow cytometry 24 hours later. Three independent transfections were performed for each experiment, and all samples were analyzed in triplicate for each transfection.

Immunoblotting

Cells were lysed in buffer containing 20 mmol/L Tris (pH 7.5), 150 mmol/L NaCl, 1% NP40, 1 mmol/L EDTA, 5 mmol/L NaF, and 5 mmol/L Na_3VO_4. Total cell lysates (30 μg) were resolved by 10% SDS-PAGE, transferred to

Published OnlineFirst October 18, 2013; DOI: 10.1158/1535-7163.MCT-13-0466

nitrocellulose membranes, and incubated with 100 to 200 μg/mL of the following antibodies: phospho-Akt (Ser473), phospho-p44/42 ERK (Thr202/Tyr204), phospho-NF-κB p65 (Ser536) and respective total kinase proteins, pro-/cleaved caspase-3, and pro-/cleaved caspase-9 (Cell Signaling Technology). For loading controls, lysates were also incubated with antibodies detecting β-actin (Sigma). Immunoreactive bands were developed using an enhanced chemiluminescence reaction (PerkinElmer).

Quantitative real-time PCR

Total RNA was isolated using the RNeasy Mini kit (Qiagen), and cDNA was synthesized from equivalent total RNA using a SuperScript III First-Strand Synthesis SuperMix Kit (Invitrogen) according to the manufacturer's instructions. Primers used for amplification of target genes are displayed in Supplementary Table S1. Amplification was carried out using an iCycler IQ Real-Time PCR Detection System, and cycle threshold (C_t) values were tabulated in duplicate for each gene of interest in each experiment. "No template" (water) controls were used to ensure minimal background contamination. Using mean C_t values tabulated for each gene, and paired C_t values for β-actin as a loading control, fold changes for experimental groups relative to assigned controls were calculated using automated iQ5 2.0 software (Bio-Rad).

Quantification of sphingolipids

Quantification of ceramide and dihydro-ceramide species was performed using a Thermo Finnigan TSQ 7000 triple-stage quadruple mass spectrometer operating in multiple-reaction monitoring positive ionization mode (Thermo Fisher Scientific). Quantification was based on calibration curves generated by spiking an artificial matrix with known amounts of target standards and an equal amount of the internal standard. The target analyte: internal standard peak area ratios from each sample were compared with the calibration curves using linear regression. Final results were expressed as the ratio of sphingolipid normalized to total phospholipid phosphate level using the Bligh and Dyer lipid extract method (34). Concentrations of S1P in ascites fluid supernatants and PEL cell lysates were determined using the S1P Assay Kit (Echelon) according to the manufacturers' instructions.

PEL xenograft model

BCBL-1 cells maintained at early passage number in cell culture were washed twice in sterile-filtered PBS before performance of trypan blue and flow cytometry assays for verification of their viability. Aliquots of 10^7 viable cells were diluted in 200 μL sterile PBS, and 6-to 8-week-old male nonobese diabetic severe-combined immunodeficient (NOD/SCID) mice (The Jackson Laboratory) received intraperitoneal injections with a single cell aliquot. For drug delivery, ABC294640 was diluted in sterile-filtered 0.375% Tween-80 (Sigma) in PBS to achieve 100 μL total volume. The drug, or vehicle alone, was administered using an insulin syringe for intraperitoneal injections, or a 20-gauge 1.0-inch animal feeding needle (Popper and Sons; item #7921) for oral gavage. Drug was administered either 1 day or 21 days after BCBL-1 injections. Three experiments, with 10 mice per group for each experiment, were performed for each route of administration. For confirmation of PEL expansion within the murine model, ascites fluid was collected 3 to 4 weeks after injection. Cells from ascites fluid were resuspended in PEL media (described earlier) for 2 hours in fibronectin-coated plates, and cells remaining in suspension were separated from adherent cells and analyzed by flow cytometry. For the latter, cells were resuspended in 3% bovine serum albumin (BSA) in 1× PBS, incubated on ice for 10 minutes, then incubated with a 1:50 dilution of primary antibodies recognizing human CD138 for an additional 30 minutes. Following two subsequent wash steps, cells were incubated for 30 minutes with goat anti-rabbit immunoglobulin G (IgG) conjugated to Alexa-647 and diluted 1:200. Control cells were incubated with secondary antibodies only. 10,000 cells were resuspended in 1× PBS for flow cytometry analysis. As a second method of validation, 10^5 nonadherent cells freshly isolated from ascites fluid cultures as earlier were placed on glass slides (using a pap pen) for 2 hours at 37°C, then incubated in 1:1 methanol:acetone at 20°C for fixation and permeabilization. Following incubation with a blocking reagent (10% normal goat serum, 3% BSA, and 1% glycine) for an additional 30 minutes, cells were incubated for 1 hour at 25°C using a 1:1,000 dilution of rat anti-LANA monoclonal antibodies (ABI), followed by 1:100 dilution of goat anti-rat secondary antibodies conjugated to Texas Red (Invitrogen). For nuclear localization, cells were subsequently counterstained with 0.5 μg/mL 4′,6-diamidino-2-phenylindole (DAPI; Sigma) in 180 mmol/L Tris-HCl (pH 7.5), washed once in 180 mmol/L Tris-HCl for 15 minutes, and prepared for visualization using a Leica TCPS SP5 AOBS confocal microscope. Weights were recorded weekly as a surrogate measure of tumor progression, and ascites fluid volumes were tabulated for individual mice at the completion of each experiment. All protocols were approved by the Louisiana State University Health Science Center Animal Care and Use Committee in accordance with national guidelines.

Immunohistochemistry

Formalin-fixed, paraffin-embedded tissues were microtome-sectioned to a thickness of 4 μm, placed on electromagnetically charged slides (Fisher Scientific), and stained with hematoxylin & eosin (H&E) for routine histologic analysis. Immunohistochemistry was performed using the Avidin-Biotin-Peroxidase complex system, according to the manufacturer's instructions (VECTASTAIN Elite ABC Peroxidase Kit; Vector Laboratories). In our modified protocol, sections were deparaffinized in xylene and rehydrated through a descending alcohol gradient. For nonenzymatic antigen retrieval, slides were heated in 0.01 mol/L sodium citrate buffer (pH 6.0) to

Published OnlineFirst October 18, 2013; DOI: 10.1158/1535-7163.MCT-13-0466

95°C under vacuum for 40 minutes and allowed to cool for 30 minutes at room temperature, then rinsed with PBS and incubated in MeOH/3% H_2O_2 for 20 minutes to quench endogenous peroxidase. Slides were then washed with PBS and blocked with 5% normal goat serum in 0.1% PBS/BSA for 2 hours at room temperature, then incubated overnight with a rat monoclonal anti-LANA antibody (ABI) using a 1:500 dilution in 0.1% PBS/BSA. The following day, slides were incubated with a goat anti-rat IgG secondary antibody at room temperature for 1 hour, followed by avidin–biotin peroxidase complexes for 1 hour at room temperature. Finally, slides were developed using a diaminobenzidine substrate, counterstained with hematoxylin, dehydrated through an ascending alcohol gradient, cleared in xylene, and coverslipped with Permount. Images were collected at ×200 and ×600 magnification using a Olympus BX61 microscope equipped with a high resolution DP72 camera and CellSense image capture software.

Isolation of circulating human B cells

Human peripheral blood mononuclear cells (PBMC) were isolated from whole blood from two healthy donors following Ficoll gradient separation. PBMC were washed and resuspended in 500 μL total volume, including 440 μL buffer composed of 2% FBS and 1 mmol/L EDTA in 1× PBS (EasySep Buffer; STEMCELL Technologies), 30 μL Fc-receptor blocker (eBiosciences), and 30 μL of a PE-conjugated anti-CD19 monoclonal antibody (BD-Pharmagen), for incubation at room temperature for 20 minutes. Of note, 100 μL EasySep PE selection cocktail (STEMCELL Technologies) was added for an additional 15 minutes, and 2.5 mL of additional buffer was then added before magnetic column separation of $CD19^+$ cells. Following column separation, supernatants were discarded and cells resuspended in fresh 2.5 mL buffer for each of two additional column separation steps. Thereafter, cells were resuspended in complete RPMI 1640 medium supplemented with 20% FBS for overnight culture with ABC294640, or in 1× PBS for flow cytometry to determine the purity of selection. For both donors, 92% to 95% pure populations of $CD19^+$ cells were recovered (data not shown).

Statistical analysis

Significance for differences between experimental and control groups were determined using the two-tailed Student *t* test (Excel 8.0), and *P* values less than 0.01 were considered significant.

Results

Pharmacologic targeting of SphK with ABC294640 results in dose-dependent induction of apoptosis for PEL cells

To first determine whether pharmacologic targeting of SPHK *in vitro* impacts metabolic activity for PEL cells, we incubated either $KSHV^+/EBV^{neg}$ BCBL-1 cells or $KSHV^{neg}/EBV^{neg}$ BL-41 cells with ABC294640 at concentrations previously shown to impact SPHK2 function, but not SPHK1 (28). We found that the drug induces significant dose-dependent suppression of metabolic activity of BCBL-1 based on MTT assays, with little or no impact on BL-41 cells (Fig. 1A). Next, using flow cytometry, we found that ABC294640 induces apoptosis in dose-dependent fashion for BCBL-1 cells, but has little impact on BL-41 cells over the same range of concentrations (Fig. 1B and C). We also found that ABC294640 induced dose-dependent apoptosis for other $KSHV^+$ PEL cell lines, including $KSHV^+/EBV^+$ BC-1 cells, $KSHV^+/EBV^{neg}$ BC-3 cells, and $KSHV^+/EBV^{neg}$ BCP-1 cells (Fig. 1D–F). Providing additional evidence for drug selectivity, we observed a lack of discernible drug-induced toxicity for primary human $CD19^+$ B cells isolated from peripheral blood of healthy donors (Supplementary Fig. S1) at concentrations commensurate with those achievable in human plasma following administration of the predicted therapeutic dose of ABC294640 (20 μmol/L or less based on the ongoing clinical trial; NCT01488513). Of note, we observed significant increases in toxicity for B-cell tumors at 20 μmol/L *in vitro* (Fig. 1).

To confirm inhibition of SPHK in cells for which ABC294640 induces appreciable toxicity, we used mass spectrometry analyses to quantify intracellular levels of bioactive ceramides and dihydro(dh)-ceramides, as well as a modified ELISA assay to quantify S1P. We observed dose-dependent accumulation of total ceramide and dh-ceramide levels, and reductions in S1P, within BCBL-1 cells in the presence of ABC294640 (Fig. 2), thereby confirming dose-dependent inhibition of SPHK function in these cells.

ABC294640 induces apoptosis for PEL cell lines through suppression of KSHV-associated signal transduction

As mentioned previously, S1P induces activation of NF-κB and MAPKs, including extracellular signal-regulated kinase (ERK), and these pathways are also activated by KSHV-encoded latent proteins and increase viability for infected cells (22, 23, 32, 35). Therefore, we sought to determine whether ABC294640 impairs constitutive signal transduction in PEL cells, and whether reversal of drug-induced suppression of these pathways restores PEL viability. We observed dose-dependent suppression of ERK, Akt, and NF-κB p65 phosphorylation, as well as cleavage of caspases-3 and 9, within BCBL-1 cells exposed to ABC294640, but not within drug-resistant BL-41 cells (Fig. 3A). To verify whether ABC294640-induced apoptosis is associated with drug-mediated suppression of signal transduction, we transiently transfected BCBL-1 cells with constructs encoding either ERK or p65 before their incubation with ABC294640. We found that overexpression of either ERK or p65 (and resultant increases in phospho-ERK/p65) partially suppressed apoptosis induced by ABC294640 (Fig. 3B and C). To validate these observations, we used RNAi targeting SPHK2 given the

Published OnlineFirst October 18, 2013; DOI: 10.1158/1535-7163.MCT-13-0466

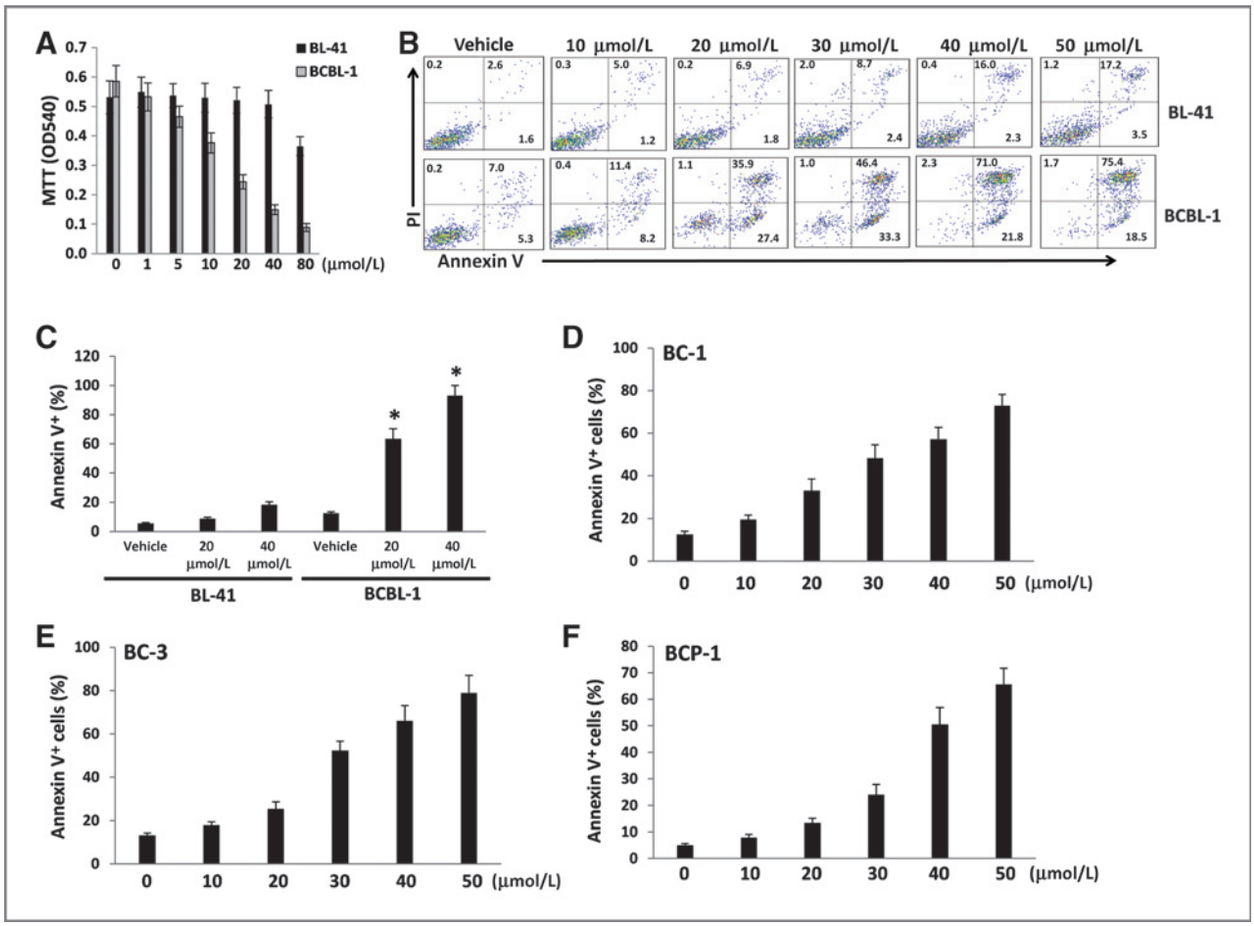

Figure 1. Pharmacologic targeting of SPHK with ABC294640 (ABC) results in dose-dependent reduction in viability and apoptosis for PEL cells. A, KSHV^{neg}/EBV^{neg} BL-41 and KSHV^{+}/EBV^{neg} BCBL-1 cells were incubated with the indicated concentrations of ABC or vehicle for 16 hours. Metabolic activity was quantified using MTT assays. B and C, BL-41 and BCBL-1 cells were treated as in A and apoptosis was quantified using flow cytometry assays as described in Materials and Methods. *, $P < 0.01$. D to F, KSHV^{+}/EBV^{+} BC-1 cells (D), KSHV^{+}/EBV^{neg} BC-3 cells (E), and KSHV^{+}/EBV^{neg} BCP-1 cells (F) were incubated with the indicated concentrations of ABC or vehicle for 16 hours and apoptosis was quantified as earlier. Error bars, SEM for three independent experiments.

preferential inhibitory activity of the drug for this isoform at the concentrations used in our studies. Achieving 60% to 70% reduction in basal SPHK2 transcript expression for BCBL-1 and BCP-1 cells using this approach (Fig. 4A and B), we found that PEL cells exhibited reduced activation of ERK, Akt, and p65 phosphorylation (Fig. 4C), as well as a 5-to 6-fold increase in apoptosis and cell death (Fig. 4D and E).

ABC294640 suppresses PEL progression and induces regression of established PEL tumors *in vivo*

As noted earlier, ABC294640 displays *in vivo* activity in preclinical tumor models (28, 29), but its activity against virus-associated tumors, and hematologic tumors generally, has not been explored. Therefore, we sought to determine the activity of ABC294640 against PEL tumors *in vivo* using an established xenograft model in which PEL cells are introduced into the peritoneal cavity of immune-compromised mice. This results in intracavitary tumor expansion with development of ascites and increases in abdominal girth associated with "free-floating" PEL cells, as well as formation of solid PEL tumors within the peritoneal cavity and distal organs following hematogenous dissemination (36, 37). We injected BCBL-1 cells into NOD/SCID mice for these experiments, given a high degree of resistance for BCBL-1 cells to conventional cytotoxic agents relative to other PEL cell lines (7), which is due in part to increased surface expression of drug efflux pumps (9). We observed clear PEL expansion within 3 to 4 weeks using our protocol, including time-dependent weight gain and increased abdominal girth, as well as ascites accumulation and splenic enlargement due to tumor infiltration at the time of necropsy (Fig. 5). These observations were validated through identification of human CD138^{+} PEL cells recovered from within ascites fluid (Supplementary Fig. S2A), as well as observation of intranuclear expression of KSHV-encoded LANA within tumor cells from ascites fluid (Supplementary Fig. S2B) and within splenic tissue (Supplementary Fig. S2C).

Published OnlineFirst October 18, 2013; DOI: 10.1158/1535-7163.MCT-13-0466

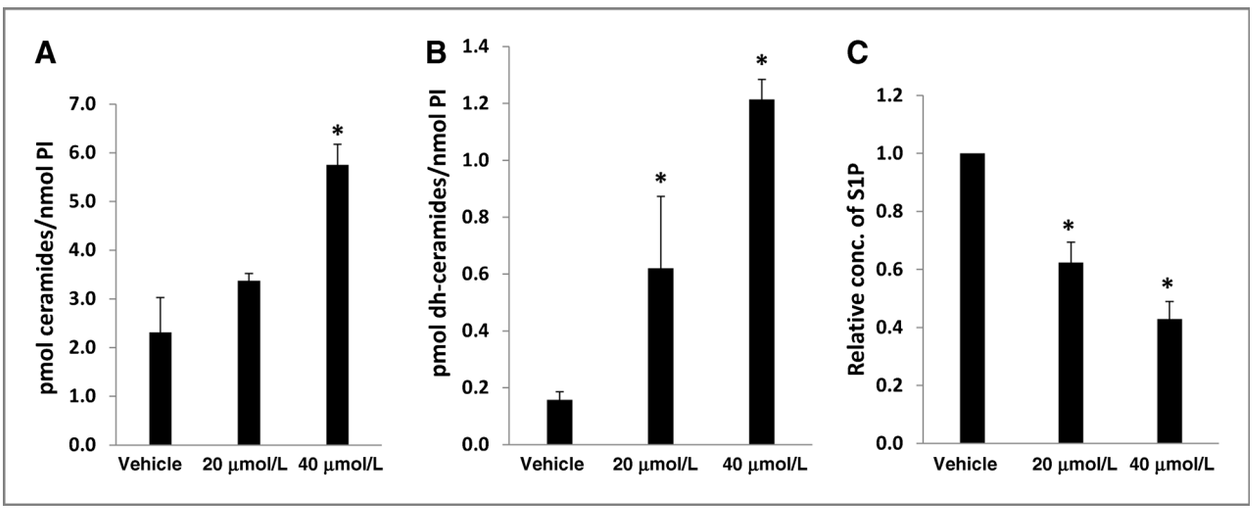

Figure 2. ABC294640 (ABC) increases accumulation of ceramide species and reduces S1P levels within PEL cells. A and B, BCBL-1 cells were incubated with the indicated concentrations of ABC or vehicle for 16 hours, then ceramide and dihydro-ceramide species were quantified as described in Materials and Methods. C, cells were treated as in A and the concentration of intracellular S1P quantified by ELISA. Error bars, SEM for three independent experiments; *, $P < 0.01$.

For initial experiments, we administered ABC294640, either intraperitoneally or orally, within 24 hours of PEL cell injections. ABC294640 significantly reduced tumor expansion with either route of administration (Fig. 5). To obtain sufficient tumor tissue for relevant *ex vivo* analyses, we performed additional experiments in which ABC294640 therapy was initiated following establishment of PEL tumors (beginning 21 days after PEL cell injections). Using this approach, drug-treated mice exhibited significant regression of PEL tumor burden relative to untreated animals (Fig. 6A–C).

Sufficient and homogenous populations of ascites-derived PEL cells were retrievable from drug-treated and untreated mice in these latter experiments for subsequent analyses (Supplementary Fig. S2). To assess SPHK inhibition in the model, lipid mass spectrometry

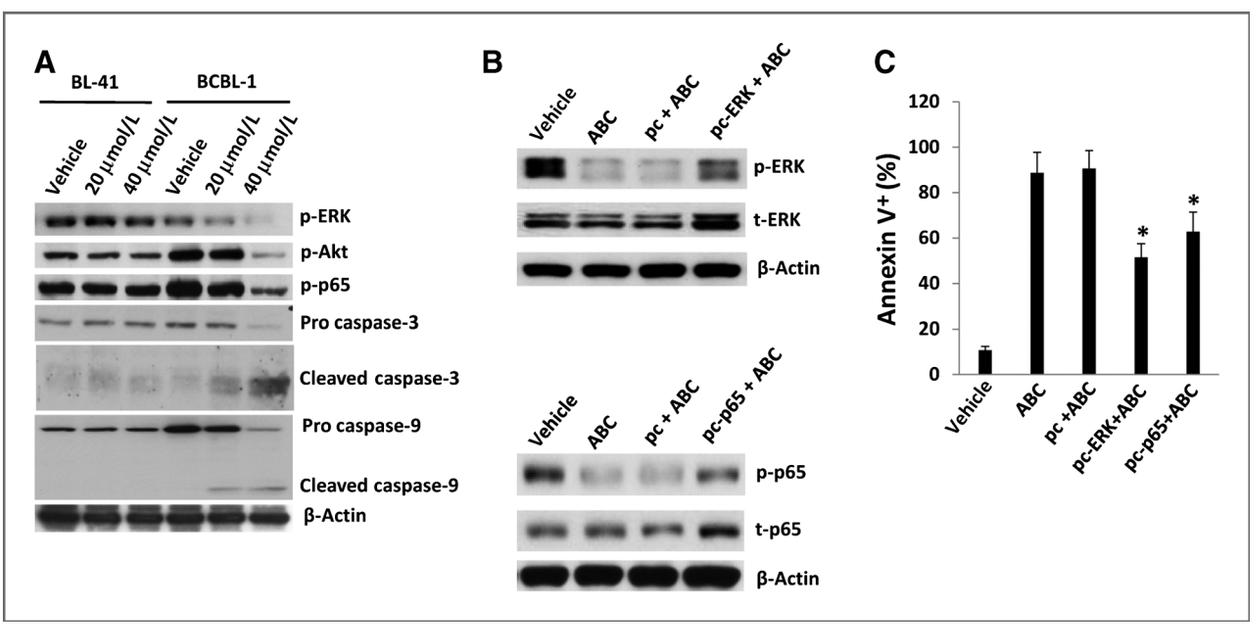

Figure 3. ABC294640 (ABC) induces apoptosis for PEL cells through suppression of intracellular signal transduction. A, BL-41 and BCBL-1 cells were incubated with the indicated concentrations of ABC or vehicle for 16 hours, and immunoblots were performed to identify phosphorylated signaling intermediates and caspase cleavage, with β-actin used as an internal control. B and C, BCBL-1 cells were transfected with control vector (pc), or vectors encoding ERK (pc-ERK) or NF-κB p65 (pc-p65) for 24 hours, then incubated with either vehicle or 40 μmol/L ABC) for an additional 16 hours. Protein expression was detected using immunoblots (B) and apoptosis was quantified using flow cytometry (C). Error bars, SEM for three independent experiments; *, $P < 0.01$.

Published OnlineFirst October 18, 2013; DOI: 10.1158/1535-7163.MCT-13-0466

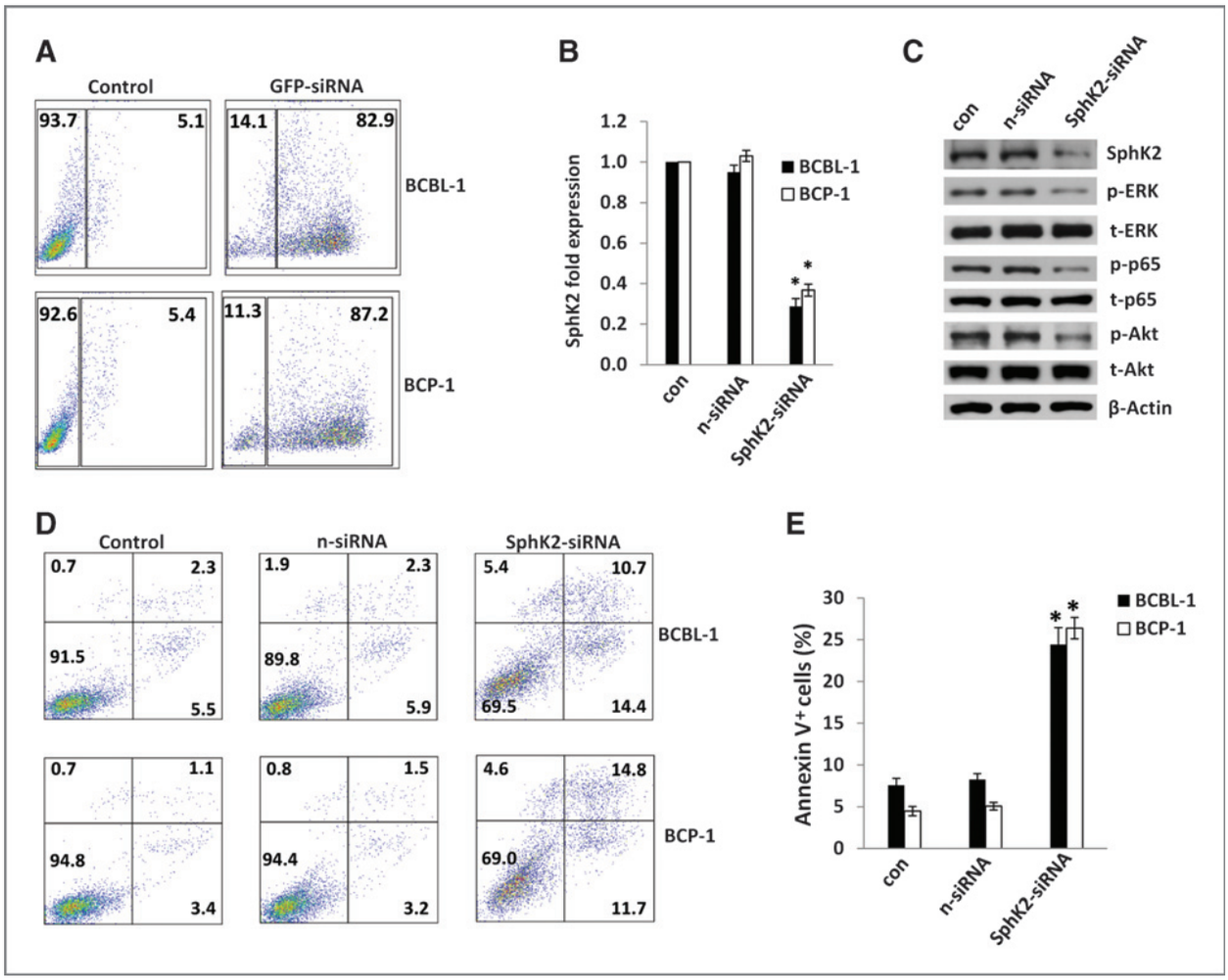

Figure 4. Targeting SPHK2 by RNAi induces PEL cell apoptosis. A, BCBL-1 and BCP-1 cells were transfected with siRNA conjugated to GFP for 24 hours and transfection efficiency was determined by flow cytometry. Data shown represent one of three independent experiments. B, BCBL-1 and BCP-1 cells were transfected with control (n-siRNA) or SPHK2-specific siRNA (SPHK2-siRNA) for 48 hours, then SPHK2 transcripts were quantified using quantitative real-time PCR (qRT-PCR). Data are normalized to nontransfected cells, and using β-actin as a loading control. C, BCBL-1 cells were treated as in B and protein expression was determined using immunoblots, including β-actin as loading control. Data shown represent one of three independent experiments. D and E, BCBL-1 and BCP-1 cells were treated as in B, and apoptosis was quantified using flow cytometry as described in Materials and Methods. Error bars, SEM for three independent experiments; *, $P < 0.01$.

was performed using ascites-derived PEL cell lysates from individual animals. Higher concentrations of ceramides and dh-ceramides were observed within live tumor cells from drug-treated animals, although these differences were not significant (Supplementary Fig. S3A and S3B). However, cells from drug-treated animals exhibited significantly reduced concentrations of intracellular S1P (Supplementary Fig. S3C). Lipid mass spectrometry performed on cell-free fluid requires large sample volumes, limiting the utility of this approach for comparison of cell-free intracavitary sphingolipid concentrations between individual animals. Nevertheless, we performed these assays after pooling cell-free ascites fluid, and we observed increases in ceramides and dh-ceramides, as well as reductions in S1P, within pooled samples from ABC294640-treated mice relative to their untreated counterparts (Supplementary Fig. S3D–S3F). Plasma-based assays were also performed, but low concentrations of bioactive sphingolipids in this compartment precluded meaningful comparisons (data not shown).

To determine whether ABC294640 induces apoptosis and suppresses KSHV-associated signal transduction for PEL cells *in vivo*, we performed immunoblot analyses using ascites-derived PEL cell lysates from representative animals. Increases in annexin expression, along with increases in caspase-3 and -9 cleavage and reductions in ERK, Akt, and p65 phosphorylation, were noted for cells from drug-treated mice (Fig. 6D and E), commensurate with our *in vitro* data. We also quantified expression of representative KSHV transcripts from ascites-derived PEL cell lysates from individual animals. We found that

Published OnlineFirst October 18, 2013; DOI: 10.1158/1535-7163.MCT-13-0466

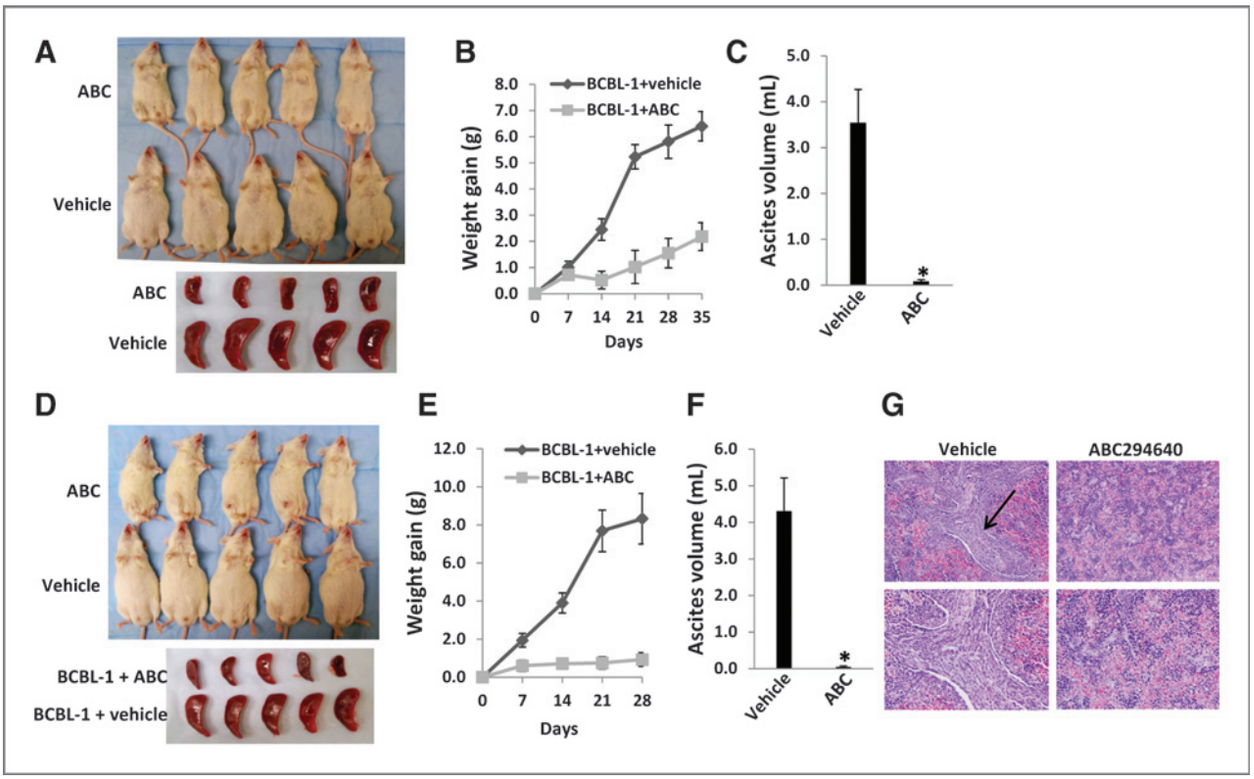

Figure 5. ABC294640 (ABC) suppresses PEL progression *in vivo*. NOD/SCID mice were injected intraperitoneally with 10^7 BCBL-1 cells. Beginning 24 hours later, 50 mg/kg ABC or vehicle ($n = 10$ per group) were administered intraperitoneally (A–C) or by oral gavage (D–F), once daily, 5 days per week, for each of three independent experiments. Weights were recorded weekly. Images of representative animals and their respective spleens, as well as ascites fluid volumes, were collected at the conclusion of experiments on day 35 (A–C) or day 28 (D–F). Error bars, SEM for three independent experiments; *, $P < 0.01$. G, spleens from vehicle- or ABC (50 mg/kg)-treated mice were prepared for routine H&E staining as described in Materials and Methods for identification of tumors infiltrating along vascular channels (arrow). Data shown represent individual animals from one of three independent experiments (×200, top; ×600, bottom).

PEL cells from drug-treated animals exhibited significantly increased expression of all lytic genes profiled, including ORF50, but no change in expression of latent ORF73 transcripts (which encode LANA; Fig. 6F). To validate these findings, we repeated *in vitro* experiments incubating BCBL-1 cells with ABC294640 and noted dose-dependent increases in expression of lytic transcripts with drug exposure, but once again no change in expression of ORF73 (Fig. 6G).

Discussion

To our knowledge, this is the first report directly implicating bioactive sphingolipids in KSHV pathogenesis. Our data are also consistent with previous reports correlating antitumor effects for ABC294640 with intratumoral accumulation of proapoptotic ceramide species, reduced S1P levels, and suppression of MAPK and NF-κB activation (28, 29, 38, 39). One recent study reported induction of autophagy within renal, prostate, and breast cancer cell lines following exposure to ABC294640, and use of an inhibitor of autophagy enabled apoptosis while reducing tumor cell death with ABC294640 exposure (40). These data suggest that for some tumors, ABC294640 may synergize with other proapoptotic agents to cause cell death through complimentary induction of autophagy. However, induction of autophagy may actually facilitate use of alternative energy sources and promote cancer-cell proliferation within established tumors (41). We found that ABC294640 induces dose-dependent apoptosis for a variety of patient-derived PEL cell lines *in vitro* and *in vivo*, and parallel experiments using ascites tumor lysates from drug-treated animals failed to reveal protein signatures consistent with activation of autophagy (data not shown). The relative importance of apoptosis and autophagy pathways for PEL cell death during ABC294640 treatment requires further clarification to inform future preclinical studies and clinical trials using combination therapies targeting these pathways.

On the basis of a wealth of published data and our own observations, suppression of constitutive signal transduction, accumulation of proapoptotic ceramides, reductions in antiapoptotic signaling associated with S1P, and/or induction of KSHV lytic gene expression may all logically contribute to PEL cell apoptosis induced by ABC294640. Restoration of ERK and p65 activation during drug

Published OnlineFirst October 18, 2013; DOI: 10.1158/1535-7163.MCT-13-0466

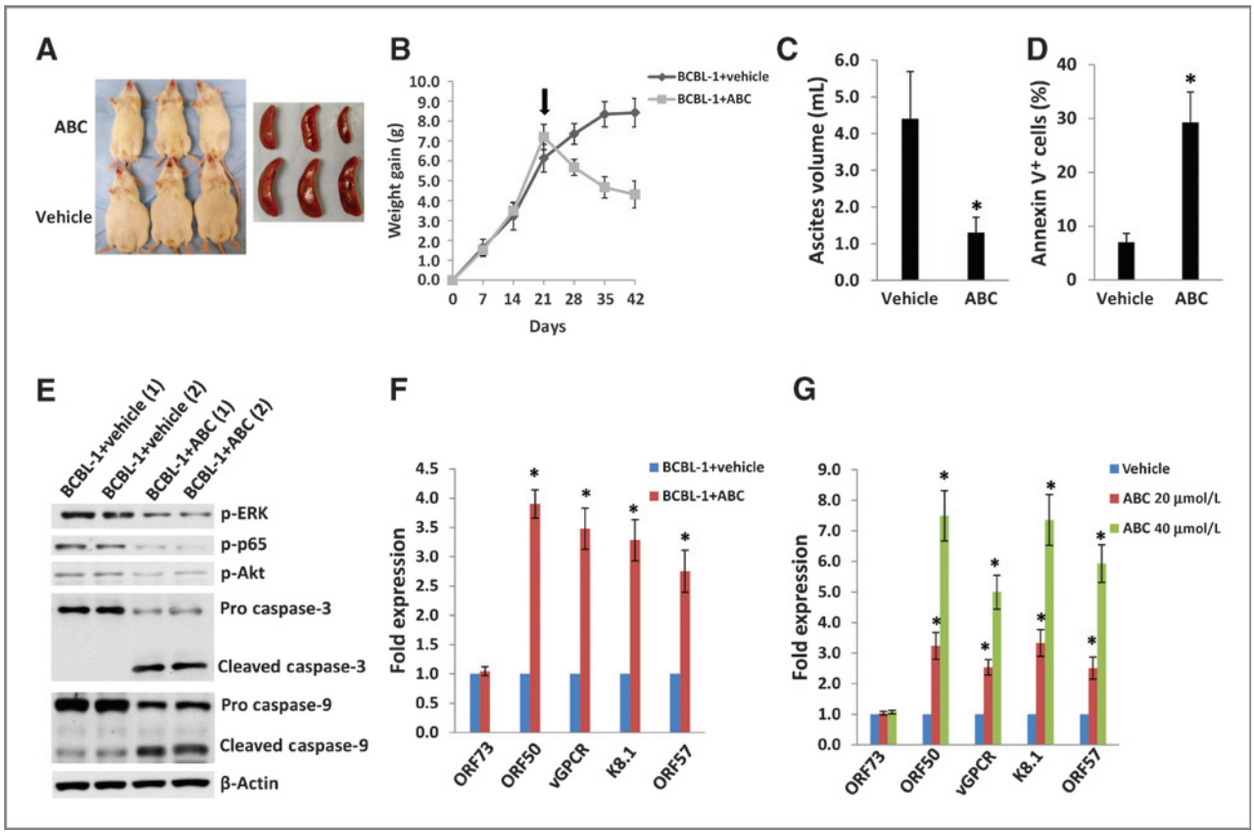

Figure 6. ABC294640 (ABC) induces regression of established PEL tumors *in vivo*. A to C, NOD/SCID mice were injected intraperitoneally with 10^7 BCBL-1 cells. Beginning 21 days later, 100 mg/kg ABC or vehicle ($n = 10$ per group) were administered intraperitoneally once daily, 5 days per week, for an additional 21 days for each of three independent experiments. Weights were recorded weekly, and images of representative animals and their respective spleens, as well as ascites fluid volumes, were collected at the conclusion of experiments on day 42. D, apoptosis was quantified by flow cytometry for live PEL cells recovered from ascites fractions as described in Materials and Methods and Supplementary Fig. S2. E, immunoblots were performed to identify phosphorylated signaling intermediates and caspase cleavage within live PEL cells recovered from ascites fractions from each of 2 mice representing vehicle- and drug-treated groups. F, RNA was recovered from live PEL cells from ascites fractions from each of 4 mice representing vehicle- or drug-treated groups, and this was done for two independent experiments. Quantitative real-time PCR (qRT-PCR) was used to quantify viral transcripts representing either latent (ORF73) or lytic genes, including the lytic "switch" gene ORF50. Data were normalized to samples representing vehicle-treated mice, and using β-actin as a loading control. G, BCBL-1 cells were incubated with the indicated concentrations of ABC or vehicle for 16 hours and representative viral transcripts quantified using qRT-PCR as earlier. Error bars, SEM for two (F) or three (B and G) independent experiments; *, $P < 0.01$.

treatment only partially restored PEL viability, and we observed coincident dose-dependent activation of viral lytic gene expression with the drug. Induction of KSHV lytic gene expression, governed by the lytic "switch" gene ORF50, typically results in PEL cell death (42–44), and this concept has been explored as a therapeutic strategy given that standard cytotoxic agents, as well as bortezomib and valproic acid [the latter a histone deacetylase (HDAC) inhibitor used for a variety of clinical applications], induce lytic gene expression and reduce PEL cell viability (36, 37, 42, 45). KSHV lytic gene expression is inhibited through HDAC binding to ORF50, (46), and viral genes expressed predominantly during lytic replication suppress HDAC activity (47). A role for SPHK in epigenetic regulation was revealed through its direct association with core histone H3 and generation of intranuclear S1P that binds active sites on HDACs to inhibit their enzymatic activity (48). These data suggest a potential role for SPHK and S1P in regulating the KSHV lytic switch. Because KSHV microRNAs also regulate the lytic switch, induce antiapoptotic signal transduction, promote viral latency, and suppress caspase-3–mediated apoptosis for KSHV-infected cells (49–53), future mechanistic studies might logically focus on whether SphK and S1P regulate KSHV microRNA expression and function. Whether the observed lack of toxicity for $KSHV^{neg}/EBV^{neg}$ BL-41 cells and human peripheral B cells isolated from healthy donors in our studies is related to the lack of established viral infection within these cells (and, by extension, lack of induction of death-associated lytic viral gene expression) requires confirmation. Additional studies are also needed to address potential mechanisms for drug resistance, including drug transporter expression or compensatory signaling associated with cellular oncogenes.

ABC294640 exhibits little or no inhibitory activity for SPHK1 at concentrations up to 100 μmol/L (28), a

Published OnlineFirst October 18, 2013; DOI: 10.1158/1535-7163.MCT-13-0466

concentration that exceeds those used in our *in vitro* studies. Moreover, we find that RNAi targeting of SPHK2 alone is sufficient to suppress ERK, Akt, and NF-κB activation and induce apoptosis for PEL cells. Induction of apoptosis with SPHK2 knockdown was incomplete, although this could reflect limitations of our assays given low-level persistence of SPHK2 transcripts and protein with our siRNA protocol. Therefore, although we feel it is unlikely that ABC294640 reduces S1P production in PEL cells through inhibition of SphK1 at clinically achievable concentrations, we cannot categorically exclude drug inhibition of SPHK1 as a mechanism for the observations in the present studies.

S1P binds to one of five G-protein–coupled S1P receptors (S1PR1–5) that activate diverse downstream signaling pathways (54). Our identification of extracellular S1P within ascites fluid from tumor-bearing mice suggests that PEL cells may support their own growth through secretion of S1P and augmentation of signal transduction through autocrine or paracrine mechanisms. Therefore, additional experiments are under way to characterize S1PR expression by PEL cells and to determine their relative importance for constitutive PEL signaling, as well as the role for exogenous S1P in survival for KSHV-infected cells. Our data also indicate that S1P may be useful as either a diagnostic tool or prognostic biomarker in ascites fluid, and future clinical trials including these assays should provide additional information.

Collectively, our data imply that SPHK (specifically SPHK2) and S1P play a role in PEL pathogenesis through regulation of well-characterized signal transduction pathways and possibly KSHV gene expression. Most importantly, our studies highlight SPHK as a potential therapeutic target for PEL and justify performance of early-phase clinical trials evaluating ABC294640 in HIV^+ patients with PEL or other aggressive B-cell lymphomas who have thus far been excluded from clinical trials with this agent.

Disclosure of Potential Conflicts of Interest

C.D. Smith is the President and Chief Executive Officer and has ownership interests (including patents) in Apogee Biotechnology Corporation. No potential conflicts of interest were disclosed by the other authors.

Authors' Contributions

Conception and design: Z. Qin, L. Dai, P. Rodriguez, C. Parsons
Development of methodology: W. Wang, P. Rodriguez, C. Parsons
Acquisition of data (provided animals, acquired and managed patients, provided facilities, etc.): Z. Qin, L. Dai, J. Trillo-Tinoco, W. Wang, L. Del Valle, P. Rodriguez, C.D. Smith, C. Parsons
Analysis and interpretation of data (e.g., statistical analysis, biostatistics, computational analysis): Z. Qin, J. Trillo-Tinoco, L. Del Valle, C. Voelkel-Johnson, C. Parsons
Writing, review, and/or revision of the manuscript: Z. Qin, T. Reske, K. Bonstaff, L. Del Valle, C. Voelkel-Johnson, C.D. Smith, C. Parsons
Administrative, technical, or material support (i.e., reporting or organizing data, constructing databases): Z. Qin, L. Dai, C. Senkal, E. Flemington, B. Ogretmen, C. Parsons
Study supervision: Z. Qin, C. Parsons

Acknowledgments

The authors thank Drs. Yusuf Hannun (Stony Brook University, NY) and Scott Eblen (Medical University of South Carolina) for providing p65 and ERK overexpression vectors, respectively.

Grant Support

This work was supported by independent grants from the NIH (CA88932 and DE16572 to B. Ogretmen, and AI087167 to C. Parsons), a Center for Biomedical Research Excellence subaward (RR021970 to Z. Qin and L. Del Valle), the SOM Research Enhancement Funding (5497400038 to Z. Qin), the National Natural Science Foundation (81272191 to Z. Qin), and the NNSF for Young Scientists of China (81101791 to Z. Qin).

The costs of publication of this article were defrayed in part by the payment of page charges. This article must therefore be hereby marked *advertisement* in accordance with 18 U.S.C. Section 1734 solely to indicate this fact.

Received June 10, 2013; revised September 27, 2013; accepted October 13, 2013; published OnlineFirst October 18, 2013.

References

1. Kaplan LD. HIV-associated lymphoma. Best Prac Res Clin Haematol 2012;25:101–17.
2. Cesarman E, Chang Y, Moore PS, Said JW, Knowles DM. Kaposi's sarcoma-associated herpesvirus-like DNA sequences in AIDS-related body-cavity-based lymphomas. N Engl J Med 1995;332:1186–91.
3. Simonelli C, Spina M, Cinelli R, Talamini R, Tedeschi R, Gloghini A, et al. Clinical features and outcome of primary effusion lymphoma in HIV-infected patients: a single-institution study. J Clin Oncol 2003;21:3948–54.
4. Navarro WH, Kaplan LD. AIDS-related lymphoproliferative disease. Blood 2006;107:13–20.
5. Boulanger E, Gerard L, Gabarre J, Molina JM, Rapp C, Abino JF, et al. Prognostic factors and outcome of human herpesvirus 8-associated primary effusion lymphoma in patients with AIDS. J Clin Oncol 2005;23:4372–80.
6. Chen YB, Rahemtullah A, Hochberg E. Primary effusion lymphoma. Oncologist 2007;12:569–76.
7. Petre CE, Sin SH, Dittmer DP. Functional p53 signaling in Kaposi's sarcoma-associated herpesvirus lymphomas: implications for therapy. J Virol 2007;81:1912–22.
8. Munoz-Fontela C, Marcos-Villar L, Hernandez F, Gallego P, Rodriguez E, Arroyo J, et al. Induction of paclitaxel resistance by the Kaposi's sarcoma-associated herpesvirus latent protein LANA2. J Virol 2008;82:1518–25.
9. Qin Z, Dai L, Bratoeva M, Slomiany MG, Toole BP, Parsons C. Cooperative roles for emmprin and LYVE-1 in the regulation of chemoresistance for primary effusion lymphoma. Leukemia 2011;25:1598–609.
10. Lim ST, Rubin N, Said J, Levine AM. Primary effusion lymphoma: successful treatment with highly active antiretroviral therapy and rituximab. Ann Hematol 2005;84:551–2.
11. Hocqueloux L, Agbalika F, Oksenhendler E, Molina JM. Long-term remission of an AIDS-related primary effusion lymphoma with antiviral therapy. AIDS 2001;15:280–2.
12. An J, Sun Y, Fisher M, Rettig MB. Antitumor effects of bortezomib (PS-341) on primary effusion lymphomas. Leukemia 2004;18:1699–704.
13. Abou-Merhi R, Khoriaty R, Arnoult D, El Hajj H, Dbouk H, Munier S, et al. PS-341 or a combination of arsenic trioxide and interferon-alpha inhibit growth and induce caspase-dependent apoptosis in KSHV/HHV-8-infected primary effusion lymphoma cells. Leukemia 2007;21:1792–801.
14. Kedes DH, Ganem D. Sensitivity of Kaposi's sarcoma-associated herpesvirus replication to antiviral drugs. Implications for potential therapy. J Clin Invest 1997;99:2082–6.
15. Neyts J, De Clercq E. Antiviral drug susceptibility of human herpesvirus 8. Antimicrob Agents Chemother 1997;41:2754–6.
16. Sin SH, Roy D, Wang L, Staudt MR, Fakhari FD, Patel DD, et al. Rapamycin is efficacious against primary effusion lymphoma (PEL)

Published OnlineFirst October 18, 2013; DOI: 10.1158/1535-7163.MCT-13-0466

cell lines *in vivo* by inhibiting autocrine signaling. Blood 2007;109: 2165–73.
17. Boulanger E, Afonso PV, Yahiaoui Y, Adle-Biassette H, Gabarre J, Agbalika F. Human herpesvirus-8 (HHV-8)-associated primary effusion lymphoma in two renal transplant recipients receiving rapamycin. Am J Transplant 2008;8:707–10.
18. Waddington TW, Aboulafia DM. Failure to eradicate AIDS-associated primary effusion lymphoma with high-dose chemotherapy and autologous stem cell reinfusion: case report and literature review. AIDS Patient Care STDs 2004;18:67–73.
19. Ogretmen B, Hannun YA. Biologically active sphingolipids in cancer pathogenesis and treatment. Nat Rev Cancer 2004;4:604–16.
20. Cuvillier O, Pirianov G, Kleuser B, Vanek PG, Coso OA, Gutkind S, et al. Suppression of ceramide-mediated programmed cell death by sphingosine-1-phosphate. Nature 1996;381:800–3.
21. Maceyka M, Payne SG, Milstien S, Spiegel S. Sphingosine kinase, sphingosine-1-phosphate, and apoptosis. Biochim Biophys Acta 2002;1585:193–201.
22. Wu W, Shu X, Hovsepyan H, Mosteller RD, Broek D. VEGF receptor expression and signaling in human bladder tumors. Oncogene 2003;22:3361–70.
23. Licht T, Tsirulnikov L, Reuveni H, Yarnitzky T, Ben-Sasson SA. Induction of pro-angiogenic signaling by a synthetic peptide derived from the second intracellular loop of S1P3 (EDG3). Blood 2003;102: 2099–107.
24. Grossmann C, Podgrabinska S, Skobe M, Ganem D. Activation of NF-kappaB by the latent vFLIP gene of Kaposi's sarcoma-associated herpesvirus is required for the spindle shape of virus-infected endothelial cells and contributes to their proinflammatory phenotype. J Virol 2006;80:7179–85.
25. Naranatt PP, Akula SM, Zien CA, Krishnan HH, Chandran B. Kaposi's sarcoma-associated herpesvirus induces the phosphatidylinositol 3-kinase-PKC-zeta-MEK-ERK signaling pathway in target cells early during infection: implications for infectivity. J Virol 2003;77: 1524–39.
26. Machesky NJ, Zhang G, Raghavan B, Zimmerman P, Kelly SL, Merrill AH Jr, et al. Human cytomegalovirus regulates bioactive sphingolipids. J Biol Chem 2008;283:26148–60.
27. Monick MM, Cameron K, Powers LS, Butler NS, McCoy D, Mallampalli RK, et al. Sphingosine kinase mediates activation of extracellular signal-related kinase and Akt by respiratory syncytial virus. Am J Respir Cell Mol Biol 2004;30:844–52.
28. French KJ, Zhuang Y, Maines LW, Gao P, Wang W, Beljanski V, et al. Pharmacology and antitumor activity of ABC294640, a selective inhibitor of sphingosine kinase-2. J Pharmacol Exp Ther 2010;333: 129–39.
29. Beljanski V, Lewis CS, Smith CD. Antitumor activity of sphingosine kinase 2 inhibitor ABC294640 and sorafenib in hepatocellular carcinoma xenografts. Cancer Biol Ther 2011;11:524–34.
30. French KJ, Schrecengost RS, Lee BD, Zhuang Y, Smith SN, Eberly JL, et al. Discovery and evaluation of inhibitors of human sphingosine kinase. Cancer Res 2003;63:5962–9.
31. Qin Z, Freitas E, Sullivan R, Mohan S, Bacelieri R, Branch D, et al. Upregulation of xCT by KSHV-encoded microRNAs facilitates KSHV dissemination and persistence in an environment of oxidative stress. PLoS Pathog 2010;6:e1000742.
32. Qin Z, DeFee M, Isaacs JS, Parsons C. Extracellular Hsp90 serves as a co-factor for MAPK activation and latent viral gene expression during de novo infection by KSHV. Virology 2010;403:92–102.
33. Defee MR, Qin Z, Dai L, Toole BP, Isaacs JS, Parsons CH. Extracellular Hsp90 serves as a co-factor for NF-kappaB activation and cellular pathogenesis induced by an oncogenic herpesvirus. Am J Cancer Res 2011;1:687–700.
34. Bielawski J, Szulc ZM, Hannun YA, Bielawska A. Simultaneous quantitative analysis of bioactive sphingolipids by high-performance liquid chromatography-tandem mass spectrometry. Methods 2006;39: 82–91.
35. Keller SA, Schattner EJ, Cesarman E. Inhibition of NF-kappaB induces apoptosis of KSHV-infected primary effusion lymphoma cells. Blood 2000;96:2537–42.
36. Sarosiek KA, Cavallin LE, Bhatt S, Toomey NL, Natkunam Y, Blasini W, et al. Efficacy of bortezomib in a direct xenograft model of primary effusion lymphoma. Proc Natl Acad Sci U S A 2010;107:13069–74.
37. Yanagisawa Y, Sato Y, Asahi-Ozaki Y, Ito E, Honma R, Imai J, et al. Effusion and solid lymphomas have distinctive gene and protein expression profiles in an animal model of primary effusion lymphoma. J Pathol 2006;209:464–73.
38. Chumanevich AA, Poudyal D, Cui X, Davis T, Wood PA, Smith CD, et al. Suppression of colitis-driven colon cancer in mice by a novel small molecule inhibitor of sphingosine kinase. Carcinogenesis 2010;31: 1787–93.
39. Antoon JW, White MD, Slaughter EM, Driver JL, Khalili HS, Elliott S, et al. Targeting NFkB mediated breast cancer chemoresistance through selective inhibition of sphingosine kinase-2. Cancer Biol Ther 2011;11:678–89.
40. Beljanski V, Knaak C, Smith CD. A novel sphingosine kinase inhibitor induces autophagy in tumor cells. J Pharmacol Exp Ther 2010;333: 454–64.
41. Maes H, Rubio N, Garg AD, Agostinis P. Autophagy: shaping the tumor microenvironment and therapeutic response. Trends Mol Med 2013;19:428–46.
42. Shaw RN, Arbiser JL, Offermann MK. Valproic acid induces human herpesvirus 8 lytic gene expression in BCBL-1 cells. AIDS 2000;14: 899–902.
43. Gwack Y, Byun H, Hwang S, Lim C, Choe J. CREB-binding protein and histone deacetylase regulate the transcriptional activity of Kaposi's sarcoma-associated herpesvirus open reading frame 50. J Virol 2001;75:1909–17.
44. Sun R, Lin SF, Gradoville L, Yuan Y, Zhu F, Miller G. A viral gene that activates lytic cycle expression of Kaposi's sarcoma-associated herpesvirus. Proc Natl Acad Sci U S A 1998;95:10866–71.
45. Lechowicz M, Dittmer DP, Lee JY, Krown SE, Wachsman W, Aboulafia D, et al. Molecular and clinical assessment in the treatment of AIDS Kaposi sarcoma with valproic acid. Clin Infect Dis 2009;49:1946–9.
46. Lu F, Zhou J, Wiedmer A, Madden K, Yuan Y, Lieberman PM. Chromatin remodeling of the Kaposi's sarcoma-associated herpesvirus ORF50 promoter correlates with reactivation from latency. J Virol 2003;77:11425–35.
47. Martinez FP, Tang Q. Leucine zipper domain is required for Kaposi sarcoma-associated herpesvirus (KSHV) K-bZIP protein to interact with histone deacetylase and is important for KSHV replication. J Biol Chem 2012;287:15622–34.
48. Hait NC, Allegood J, Maceyka M, Strub GM, Harikumar KB, Singh SK, et al. Regulation of histone acetylation in the nucleus by sphingosine-1-phosphate. Science 2009;325:1254–7.
49. Lei X, Bai Z, Ye F, Xie J, Kim CG, Huang Y, et al. Regulation of NF-kappaB inhibitor IkappaBalpha and viral replication by a KSHV microRNA. Nat Cell Biol 2010;12:193–9.
50. Liang D, Gao Y, Lin X, He Z, Zhao Q, Deng Q, et al. A human herpesvirus miRNA attenuates interferon signaling and contributes to maintenance of viral latency by targeting IKKepsilon. Cell Res 2011;21:793–806.
51. Gottwein E, Cullen BR. A human herpesvirus microRNA inhibits p21 expression and attenuates p21-mediated cell cycle arrest. J Virol 2010;84:5229–37.
52. Bellare P, Ganem D. Regulation of KSHV lytic switch protein expression by a virus-encoded microRNA: an evolutionary adaptation that fine-tunes lytic reactivation. Cell Host Microbe 2009;6:570–5.
53. Suffert G, Malterer G, Hausser J, Viiliainen J, Fender A, Contrant M, et al. Kaposi's sarcoma herpesvirus microRNAs target caspase 3 and regulate apoptosis. PLoS Pathog 2011;7:e1002405.
54. Strub GM, Maceyka M, Hait NC, Milstien S, Spiegel S. Extracellular and intracellular actions of sphingosine-1-phosphate. Adv Exp Med Biol 2010;688:141–55.

Published OnlineFirst October 18, 2013; DOI: 10.1158/1535-7163.MCT-13-0466

Molecular Cancer Therapeutics

Targeting Sphingosine Kinase Induces Apoptosis and Tumor Regression for KSHV-Associated Primary Effusion Lymphoma

Zhiqiang Qin, Lu Dai, Jimena Trillo-Tinoco, et al.

Mol Cancer Ther 2014;13:154-164. Published OnlineFirst October 18, 2013.